Polarization of 40-MeV Protons by Complex Nuclei*

C. F. HWANG,† G. CLAUSNITZER,‡ D. H. NORDBY, S. SUWA,§ AND J. H. WILLIAMS
School of Physics, University of Minnesota, Minneapolis, Minnesota
(Received 13 May 1963)

The polarization of 40-MeV protons scattered by helium, lithium, carbon, aluminum, nickel, and lead has been measured using a polarized proton ion source in conjunction with the Minnesota Proton Linear Accelerator. Experimental procedures utilized in the measurements are discussed in detail. p-α polarization measurements are compared with the theoretical predictions by Gammel and Thaler.

I. INTRODUCTION

IN recent years, many proton-nucleus polarization measurements at a variety of energies have been obtained.[1–24] The analyses of these polarization data with their corresponding differential cross-section results yielded phase shifts of the partial wave pertinent to the interaction at the specific energy at which these measurements were made. Examination of polarization measurements cited in the references shows that with the exception of Ref. 24 and a few points in the forward angles at[7] 66 and[23] 57 MeV, all other measurements are made at energies above 95 MeV or below 22 MeV. A paucity of polarization data exists at intermediate energies since polarization measurements require the incoming proton beam to be polarized at some stage of the experiment, and until recently there existed no convenient means to produce a polarized proton beam at intermediate energies, as contrasted with the situation for higher or lower energies.

Polarization is customarily measured by double scattering of an unpolarized beam. Let P_1 be the polarization of the beam after first scattering and A_2 be the analyzing power of the second scattering, then the asymmetry observed after the second scattering is

$$\epsilon=(L-R)/(L+R)=P_1A_2, \tag{1}$$

where L and R are the number of protons scattered to the left and right, respectively, in the second scattering. For strong interactions, it has been shown empirically[25,26] that the polarization in the second scattering, P_2, equals A_2 even if target spin is nonzero. Thus, Eq. (1) can be written as

$$\epsilon=(L-R)/(L+R)=P_1P_2, \tag{2}$$

whence

$$P_2=\epsilon/P_1=(1/P_1)((L-R)/(L+R)). \tag{3}$$

Equation (3) shows that it is possible to measure polarization at a given energy and angle by the single scattering of a polarized beam of known polarization P_1 independent of the methods used to produce the polarized beam. One notes that the validity of Eqs. (2) and (3) depends upon whether the interaction is time-reversal invariant. This assumption may or may not be valid for the inelastically scattered protons. Therefore, our results on $C^{12}(p,p')C^{12*}(Q=-4.43$ MeV) and $Li^7(p,p')Li^{7*}(Q=4.6$ MeV) are, strictly speaking, asymmetry (A_2) instead of polarization (P_2) measurements.

* Work supported in part by the U. S. Atomic Energy Commission.
† Present address: Department of Physics, Northwestern University, Evanston, Illinois.
‡ Present address: Department of Physics, University of Erlangen, Erlangen, Germany.
§ On leave from University of Tokyo, Tokyo, Japan; present address: Argonne National Laboratory, Argonne, Illinois.

[1] K. Strauch, Phys. Rev. **99**, 150 (1955).
[2] Owen Chamberlain, Emilio Segrè, Robert D. Tripp, Clyde Wiegand, and Thomas Ypsilantis, Phys. Rev. **102**, 1659 (1956).
[3] W. G. Chesnut, E. M. Hafner, and A. Roberts, Phys. Rev. **104**, 449 (1956).
[4] H. Tyrén, P. Hillman, and A. Johansson, Nucl. Phys. **3**, 336 (1957).
[5] R. Alphance, A. Johannson, and G. Tibell, Nucl. Phys. **3**, 185 (1957); **4**, 672 (1957).
[6] J. M. Dickson and D. C. Salter, Nuovo Cimento **6**, 235 (1957).
[7] A. M. Cormack, J. N. Palmieri, N. F. Ramsey, and Richard Wilson, Phys. Rev. **115**, 599 (1959).
[8] M. Heusinkveld and G. Freier, Phys. Rev. **85**, 80 (1952).
[9] A. C. Juveland and W. Jentschke, Z. Phys. **144**, 521 (1956).
[10] Karl W. Brockman, Jr., Phys. Rev. **110**, 163 (1958).
[11] M. J. Scott, Phys. Rev. **110**, 1398 (1958).
[12] W. A. Blanpied, Phys. Rev. **113**, 1099 (1959); **116**, 738 (1959).
[13] R. E. Warner and W. P. Alford, Phys. Rev. **114**, 1338 (1959).
[14] J. X. Saladin and P. Marmier, Helv. Phys. Acta **33**, 299 (1960).
[15] Suppl. Helv. Phys. Acta **6**, Chap. III (1961). This reference summarizes the p-nucleus polarization work at energy less than 25 MeV through June, 1960.
[16] J. Sanada, K. Nisimura, S. Suwa, I. Hayashi, K. Fukunage, N. Ryu, and M. Seki, J. Phys. Soc. Japan **15**, 754 (1960).
[17] S. Yamabe, M. Kondo, S. Kato, T. Yamajaki, and J. Ruan, J. Phys. Soc. Japan **15**, 2154 (1960).
[18] L. Rosen, J. E. Brolley, Jr., and L. Stewart, Phys. Rev. **121**, 1423 (1961); L. Rosen, J. E. Brolley, Jr., M. L. Gursky, and L. Stewart, *ibid.* **124**, 199 (1961).
[19] D. Hoare, A. B. Robbins, and G. W. Greenlees, Proc. Phys. Soc. (London) **77**, 830 (1961).
[20] S. Suwa, J. Sanada, K. Nisimura, J. Hoyashi, N. Ryu, and H. Hasel, University of Tokyo Report INSJ-36, 1961 (unpublished).
[21] S. J. Moss, R. I. Brown, D. G. McDonald, and W. Haeberli, Bull. Am. Phys. Soc. **6**, 226 (1961). R. I. Brown (private communication).
[22] A. B. Robbins, K. A. Grotowski, and G. W. Greenlees, in *Proceedings of the Rutherford Jubilee International Conference*, edited by J. E. Birks, (Heywood and Company Ltd., Manchester, 1962).
[23] S. Yamabe, M. Takeda, M. Kondo, S. Kato, T. Yamazaki, N. Takahashi, N. Kawai, and R. Chiba, J. Phys. Soc. Japan **17**, 729 (1962).
[24] R. M. Craig, J. C. Dore, G. W. Greenlees, J. S. Lilley, and P. C. Rowe, Phys. Letters **3**, 301 (1963).
[25] L. Rosen and J. E. Brolley, Jr., Phys. Rev. Letters **2**, 98 (1959).
[26] C. F. Hwang, T. R. Ophel, E. H. Thorndike, and Richard Wilson, Phys. Rev. **119**, 352 (1960).

Wolfenstein,[27] and Critchfield and Dodder[28] showed that from a knowledge of phase shifts calculated from differential cross sections alone (a possibility that is quite plausible at low energies where S and P waves dominate), a prediction of polarization is possible. This approach was employed successfully by Brockman[10] and was further applied by Gammel and Thaler.[29] The latter authors used all available experimental p-He scattering information including both the differential cross section measurements and the polarization results of Brockman.[10] From these measurements they determined the phase shifts for low energy p-He interactions. The measurements of Brussel and Williams[30] were then used to calculate the phase shifts of p-He scattering at 40 MeV. They demanded these phase shifts to vary smoothly in energy and to blend into the lower energy phase shifts previously determined. Finally, they predicted the p-He polarization at 40 MeV. In the absence of actual measurements, these calculated polarization results represented the best available information on the subject.

Greenlees[31] found, however, that the dependence of polarization and differential cross section upon phase shifts are sufficiently different so that phase shifts obtained from differential cross section alone is not adequate to guarantee a unique prediction of polarization. Furthermore, it has been demonstrated in p-p scattering[26] that energy extrapolation of phase shifts are not to be taken seriously. Thus, it seemed desirable to measure polarization of p-nucleus interaction at intermediate energies.

II. EXPERIMENTAL METHOD

In this section, we shall discuss the experimental techniques used in these experiments. They are, in the order to be discussed, the polarized ion source, the measurement of beam polarization, beam monitoring, detectors and associated electronics, targets and backgrounds, asymmetry measurements, and spurious asymmetries.

The Polarized Proton Ion Source

A detailed description of the Minnesota Linear Accelerator Polarized Ion Source is given in a separate article by one of the authors.[32] The following improvements upon the source have since then been incorporated. By replacing the tungsten filaments in the electron-bombardment ionizer with oxide-coated filaments and by adding air cooling of the ionizer chamber, the operating pressure of the ionizer was reduced to 2×10^{-7} Torr. Since the background ions are not polarized and their presence dilutes the protons from the polarized atomic beam, this reduction of ionizer pressure resulted in an enhancement of beam polarization to approximately 35%.

The stray field in the ionizing region was reduced to 0.1–0.6 G by adding extra magnetic shielding between the ionizer and its VacIon pumps. Consequently, it is possible to use lower values of guide field in the ionizing region. Since theoretical polarization of 50% for this source will decrease to 46% at a 20 G guide field, a lower (4–6 G) guide field served to further enhance the observed beam polarization. Moreover, lower guide fields correspond to smaller Lorentz forces exerted by the guide field upon the ions, which means a smaller influence upon the trajectory of the ions. Thus, the change of beam intensity is minimized as the lower guide field is being reversed to produce a reversal in beam polarization. With a typical guide field of 4–6 G, the beam intensity was found to change by only 20% when the guide field was reversed. Beam polarization for these values of guide field was found to be independent of small changes of the magnitude and of the sense of the guide field.

Improvements of a minor nature were also made on the dissociator. A stable hydrogen flow system, the impedance matching of the rf discharge, and remote control of the ionizer power supply were installed. With the above improvements, it is currently possible to produce a stable polarized proton beam with an intensity of 1.5×10^{7} protons/sec at 10 MeV, 2×10^{6} protons/sec at 40 MeV and a typical beam polarization of 35%.

Measurement of Beam Polarization

To determine the degree of polarization produced by the polarized ion source, the protons extracted from the ionizer were accelerated to 10 MeV where the characteristics of this polarized proton beam were studied with a He^4-polarimeter. This polarimeter consists of a collimating system to define the 10-MeV polarized beam after it leaves the quadrupole magnets, a helium gas cell target which can be pressurized up to five atmospheres absolute and cooled by liquid nitrogen to approximately 150°K to enhance counting rate, and a pair of telescopes with identical defining slits and plastic scintillating crystals placed symmetrically to the incoming beam at a fixed angle of 40° in the laboratory system. Figures 1 and 2 depict, respectively, the schematic arrangement of the polarimeter and the gas cell target with the target cooling provision.

The scattering efficiency of the polarimeter is approximately 5×10^{-7} at a scattering angle of 40° lab when the gas target is at one atm absolute and 300°K. The azimuthal angular resolution of the detector was $\pm2.5°$, and the inherent spurious asymmetry of the polarimeter was measured to be less than 1% absolute which is small in comparison to the statistical errors in the measured asymmetries.

Beam polarization (P_b) was calculated from the meas-

[27] L. Wolfenstein, Phys. Rev. **75**, 1664 (1949).
[28] C. L. Critchfield and D. C. Dodder, Phys. Rev. **76**, 602 (1949).
[29] J. L. Gammel and R. M. Thaler, Phys. Rev. **109**, 2041 (1958).
[30] M. K. Brussel and J. H. Williams, Phys. Rev. **106**, 286 (1957).
[31] G. W. Greenlees (private communication).
[32] G. Clausnitzer, Nucl. Instr. Methods (to be published).

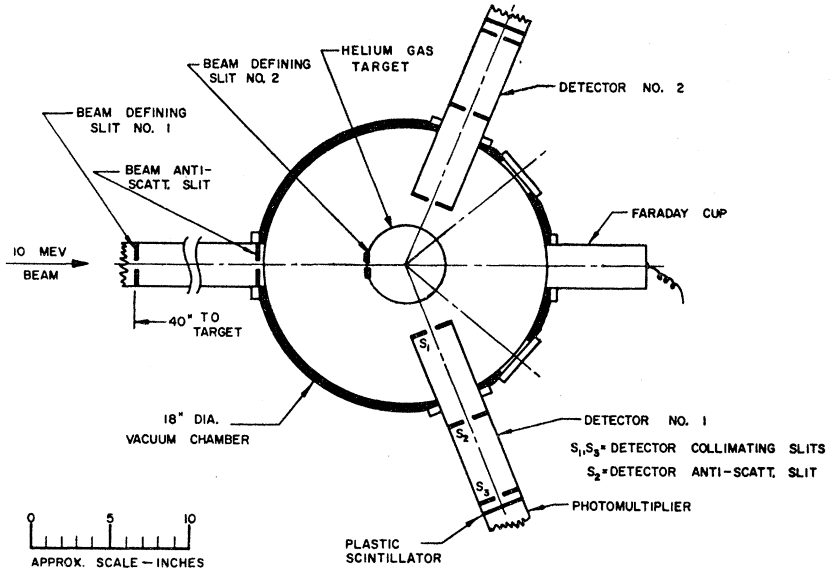

FIG. 1. Schematic diagram of p-α polarimeter.

ured asymmetries by using the p-He polarization data of Rosen *et al.*,[18] interpolated to the appropriate angle of 40° lab, ($P_2=44\%\pm5\%$). P_b was found to vary from 25% to 39% depending upon the operating conditions of the ion source. Recent measurements at Wisconsin[33] suggest that the interpolated P_2 may be too high by 10%. Recalibration of the beam polarization is now underway. Since the measured asymmetries of p-nucleus scattering will be presented herein together with calculated polarization, a recalculation of p-nucleus polarization can be readily carried out if the situation warrants.

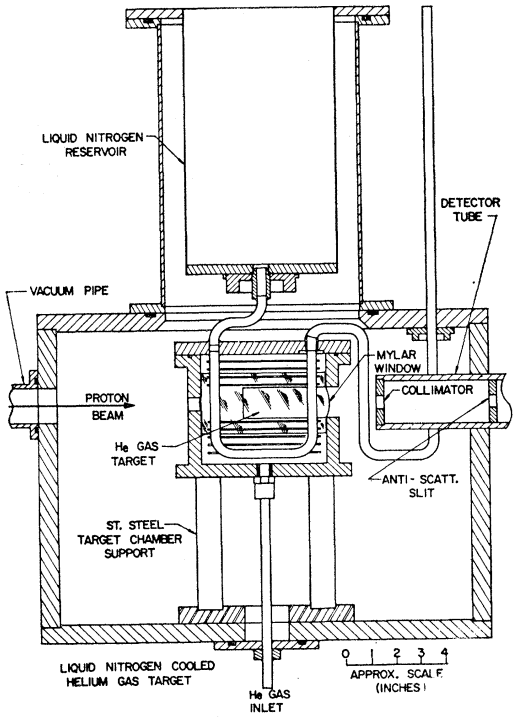

FIG. 2. Schematic diagram of liquid nitrogen cooled helium gas target.

A secondary standard of beam polarization was established by measuring the beam intensities with the sextupole magnet on and off. The beam polarization can be approximated by

$$P_b=\tfrac{1}{2}\left[1-\frac{I(\text{Magnet off})}{I(\text{Magnet on})}\right], \tag{4}$$

where the I's are the observed beam intensities and the factor $\frac{1}{2}$ arises from the theoretical value of polarization in the atomic beam. Such values of P_b were taken frequently and the averaged results were compared with the values of P_b as measured by the polarimeter. P_b as measured by the two methods were found to be in excellent agreement at 10 MeV.[34] As an additional check on the validity of this secondary method of P_b determination, the polarization of p nitrogen scattering at 10 MeV was measured using the polarimeter. P_b was calculated on the basis of the magnet on/off ratio and the polarization of p nitrogen at 40° lab was found to be $52\%\pm7\%$. This value compares well with the measurement of Rosen *et al.*[18] of $56\%\pm5\%$ interpolated to 40° lab. The P_b determination by magnet on/off ratio was used exclusively for the 40 MeV experiments for obvious reasons.

Beam Monitoring

Since it is not necessary to know the absolute beam intensities in asymmetry measurements, an air filled

[33] R. Brown (private communication).

[34] Minnesota Linear Accelerator Annual Progress Report, (1961), p. 73 (unpublished).

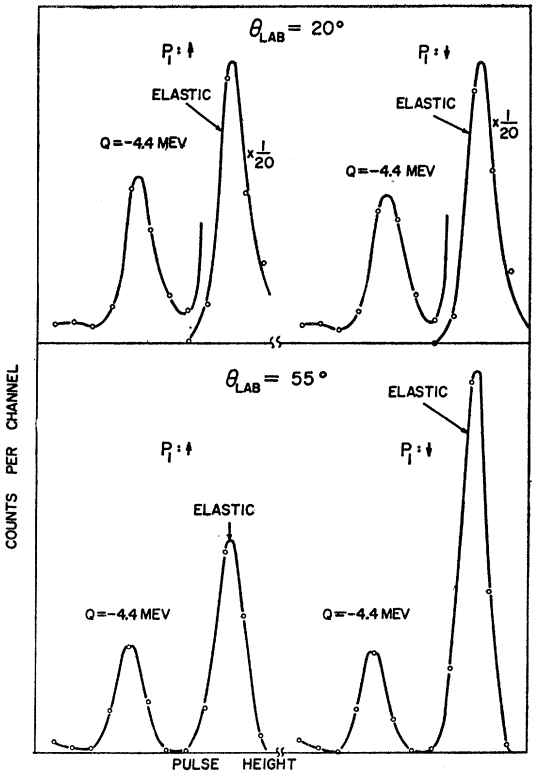

FIG. 3. Typical energy spectra of rectangular detectors from p-carbon scattering.

ionization chamber was used to monitor the polarized proton beam. The charge collected by the ionization chamber was integrated by an electrometer tube and associated circuits. Relative intensities at a fixed scattering angle so measured were found to be accurate to 0.1%.

Detectors and Associated Electronics

The proton nucleus polarization experiment apparatus utilizes a pair of 0.75 in.×3.25 in.×0.625 in. NaI(Tl) scintillation crystals mounted with their associated defining slits, light pipes, photomultipliers, and preamplifiers on the movable arms of a 1 8 ft-diam scattering stand located in the 40-MeV experimental area. These crystals subtend a solid angle of 7×10^{-3} sr at the target and have an azimuthal angular resolution of $\pm2°$.

Lucite light pipes and DuMont 6292 photomultipliers were used. Pulses were amplified, integrated, and energy analyzed by a 22-channel pulse-height analyzer. The energy spectrum of the protons scattered by carbon and detected by the rectangular NaI crystal is shown in Fig. 3. The figure shows that the system is adequate to resolve the protons from $C^{12}(p,p)C^{12}$ and $C^{12}(p,p')C^{12*}$ ($Q=-4.43$ MeV) reaction. Polarization of protons scattered by helium, lithium, carbon, aluminum, nickel, and lead were measured with these detectors.

For polarization of protons scattered by Li^6, since the first excited state of Li^6 is only 2.18 MeV above the ground state, the rectangular detectors were not adequate to resolve this first excited state. A pair of 1.5-in.-diam×0.75-in.-thick NaI (Tl) were polished and mounted. Figure 4 shows some typical energy spectra of protons scattered by Li^6 and detected by these circular detectors used in conjunction with a Nuclear Data 1024 channel pulse-height analyzer.

Targets and Background

The choice of target elements has been limited to those nuclei whose differential cross section at 40 MeV have already been measured in order to facilitate data analysis. The target elements measured were natural helium, lithium, carbon, aluminum, nickel, lead, and isotopically pure Li^6(99.37 Li^6 and 0.7% Li^7). All solid targets, having thicknesses of between 1.25 and 5 MeV, were mounted on target frames provided for the 8-ft scattering stand. In the helium measurements, a liquid-helium target was used. The target container was a 1.7-cm-diam×4-cm-high cylinder made of 0.001-

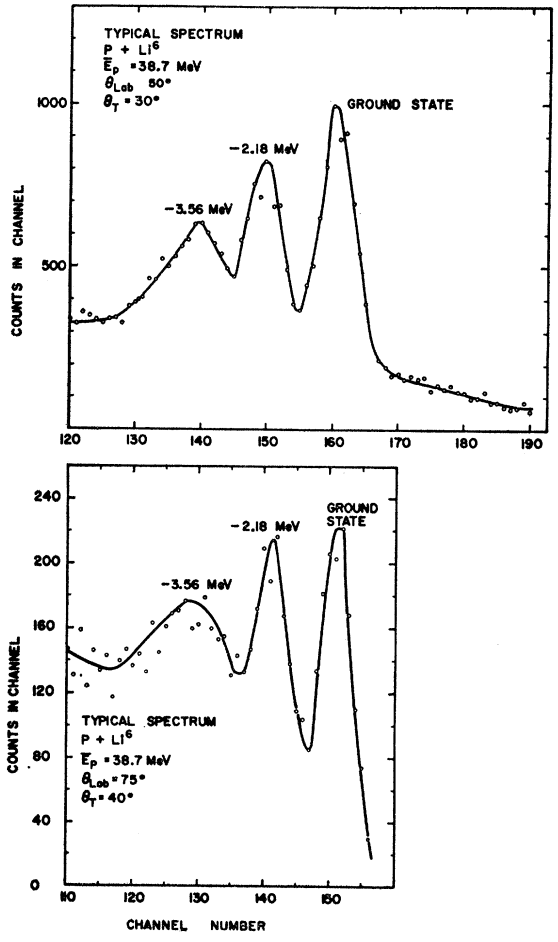

FIG. 4. Typical spectra of circular detectors.

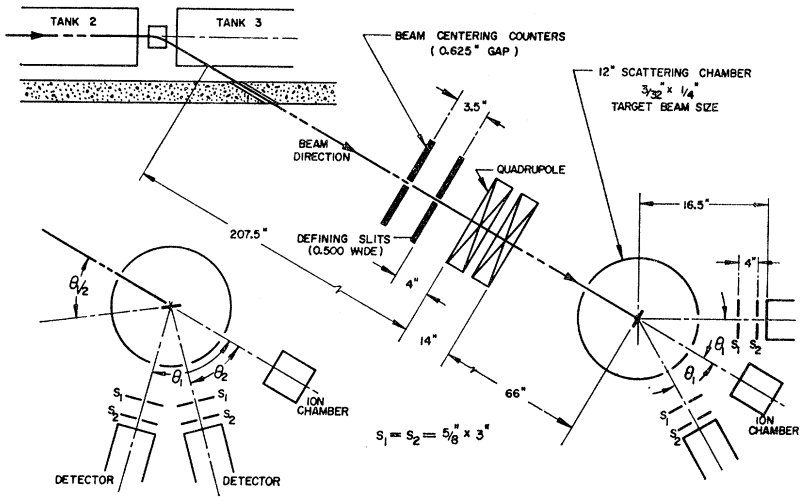

FIG. 5. Schematic diagram for the polarization experiments.

in.-thick Mylar. Construction of the target and the associated cryogenic equipment were identical to the liquid hydrogen target described in Ref. 26.

There was no measureable background for solid targets. The liquid helium target container contributed a background of 2–9%, depending upon scattering angle. Background contributions at each scattering angle from helium were measured and the measured backgrounds were subtracted from the raw counts at the appropriate angles.

Measurement of Asymmetry

In the conventional procedure of measuring asymmetry the detector is moved from time to time from one side of the beam to the other at a given angle. However, one recognizes that those protons with spin up (down) and scattered to the right (left) are exactly equivalent to those protons with spin down (up) and scattered to the left (right). Hence, the scattering of a polarized proton beam is symmetrical to a 180° rotation about the beam. Since provisions have been made in the polarized proton ion source so that the orientation of the beam polarization can be easily reversed (see section on polarized proton ion source), it is convenient to measure asymmetry by reversing beam polarization instead of moving detectors.

A schematic diagram of the proton-nucleus polarization experimental apparatus is shown in Fig. 5. The 40-MeV proton beam of the Minnesota Linear Accelerator was magnetically deflected at the exit of the second tank into the 40-MeV experimental area and was focused by a pair of magnetic quadrupole lens to a spot $\frac{3}{32}$ in. wide$\times\frac{1}{4}$ in. high at the target located at the center of the 8-ft scattering stand. Detectors were placed one on each side of the incoming proton beam at equal scattering angles. With the target perpendicular to the incoming beam, counts were obtained in each detector for both incoming protons with spins up and down. This detector configuration will be referred as mode I of data taking and is shown in the principal part of Fig. 5.

Denoting those counts obtained by the left (right) detector with incoming proton spin up and down as L^U and $L^D(R^U$ and $R^D)$, respectively, the measured asymmetry and its statistical error are then given by

$$\epsilon=(L^U+R^D-L^D-R^U)/(L^U+R^D+L^D+R^U)=P_bP_2 \quad (5)$$

and

$$\Delta\epsilon\cong 1/(L^U+R^D+L^D+R^U)^{1/2}. \quad (6)$$

Measurement of asymmetries by reversing beam polarization has three additional advantages. Firstly, if two detectors are used simultaneously, it is possible to collect two sets of data at the same time, an important advantage since counting rates for these polarization measurements are usually low. Secondly, proper combination of counts in the manner described by Eq. (5) minimizes errors in asymmetry due to misalignment of the beam, counting efficiency variation in the detectors, and beam intensity monitoring. Thirdly, at large angles when counting rates are extremely low, a convenient compromise can be realized between counting rate and energy resolution by placing the target at an appropriate angle to the incoming proton beam. This rotation of target at large scattering angles is essential in order to minimize the energy spread in the protons scattered by different portions of the target.

When the target angle is not placed at 90° to the incoming proton beam, mode I of data taking is no longer feasible. Mode II consists of placing both detectors on the same side of the incoming proton beam but at two different scattering angles, and the detector configuration of this mode of data taking is shown in the insert of Fig. 5. Let U and D be counts obtained by a given detector with incoming proton spin up and down, respectively, asymmetry is then

$$\epsilon=(U-D)/(U+D)=P_bP_2 \quad (7)$$

and

$$\Delta\epsilon\cong 1/(U+D)^{1/2}. \quad (8)$$

Since mode II of data taking is more susceptible to errors in beam intensity monitoring and to the degree of spin reversal achieved in the beam polarization, mode I of data taking was used whenever feasible. In general, small angles ($<60°$ lab) results were taken in mode I and large angles ($>50°$ lab) results were taken in mode II with overlapping angles. However, by analyzing the data, it was confirmed that mode II is no worse than mode I to within the statistical error.

Spurious Asymmetries

In order to determine the causes and magnitudes of spurious asymmetries inherent in the experimental apparatus, the unpolarized 40-MeV proton beam was scattered by the apparatus using a lead target and a scattering angle of 50° lab. Lead at 50° lab was chosen for its large $(d/d\theta)(d\sigma/dw)$, which emphasizes spurious asymmetry due to angular misalignment.

It was found that there were two major sources of spurious asymmetries. Firstly, the asymmetry measured depended upon the ability to clearly distinguish the elastically scattered protons from inelastically scattered protons. Secondly, there was a contribution of spurious asymmetry due to the random wandering of the incoming proton beam. This beam wandering was caused by the slight changes of beam energy due to the varying tuning conditions of the linear accelerator.

The first cause of spurious asymmetry is minimized by improving the resolution of energy spectrum in the detector. To minimize the spurious asymmetry contribution due to beam wandering, a pair of beam centering electrodes were placed at the entrance to the quadrupole lens. By fixing the beam position at the midpoint of the centering electrodes and holding the beam bending magnet current constant, the random beam wandering was greatly reduced.

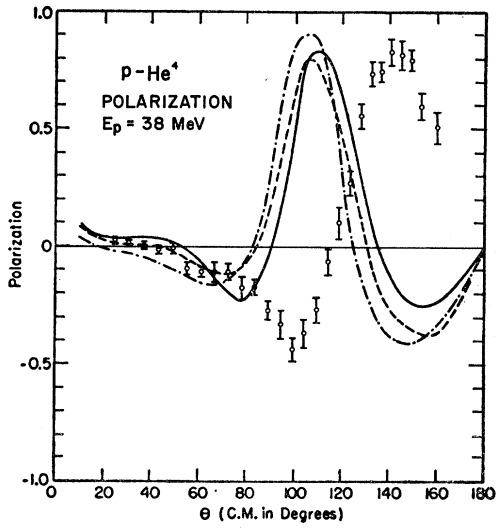

FIG. 6. p+He^4 polarization, $\bar{E}_p=38$ MeV, elastic scattering.

TABLE I. p+He polarization.

θ_{lab}(deg)	$\theta_{c.m.}$(deg)	ϵ	P_B	$\bar{E}_p=38$ MeV P_2
20	24.9	0.001±0.005	0.336	0.003±0.015
25	31.0	0.007±0.003	0.332	0.021±0.009
30	37.2	0.002±0.006	0.330	0.007±0.017
35	43.3	−0.003±0.007	0.312	−0.009±0.021
40	49.3	−0.001±0.008	0.331	−0.003±0.023
45	55.2	−0.029±0.008	0.320	−0.091±0.026
50	61.1	−0.036±0.007	0.329	−0.110±0.021
55	66.8	−0.032±0.013	0.271	−0.118±0.048
60	72.5	−0.034±0.011	0.333	−0.102±0.034
65	78.1	−0.053±0.013	0.304	−0.175±0.044
70	83.6	−0.053±0.011	0.324	−0.163±0.034
75	89.0	−0.098±0.015	0.365	−0.268±0.041
80	94.3	−0.112±0.019	0.340	−0.329±0.056
85	99.4	−0.147±0.015	0.336	−0.437±0.045
90	104.5	−0.128±0.019	0.349	−0.367±0.055
95	109.4	−0.094±0.018	0.354	−0.265±0.051
100	114.3	−0.023±0.020	0.365	−0.063±0.055
105	119.0	0.033±0.022	0.322	0.102±0.068
110	123.6	0.090±0.016	0.333	0.270±0.048
115	128.1	0.193±0.016	0.346	0.557±0.046
120	132.5	0.251±0.017	0.344	0.730±0.050
125	136.8	0.259±0.014	0.351	0.738±0.040
130	141.1	0.273±0.018	0.332	0.824±0.054
135	145.2	0.304±0.022	0.375	0.810±0.059
140	149.3	0.294±0.016	0.371	0.729±0.044
145	153.3	0.223±0.022	0.376	0.594±0.058
150	157.2	0.192±0.067	0.379	0.507±0.067

The spurious asymmetry of the apparatus after the installation of the beam centering electrodes was found to be less than 1%, a value considerably smaller than the uncertainty due to counting statistics in most cases. Also, the error caused by this asymmetry could be reduced by repeating short runs with spin up and down alternately for the same angle.

III. RESULTS

Proton-nucleus polarization versus scattering angles for helium, lithium, carbon, aluminum, nickel, lead, and Li^6 at a mean proton energy near 38 MeV are tabulated in Tables I through VII. The sense of polarization is in

TABLE II. p+Li^6 polarization elastic scattering.

θ_{lab}	$\theta_{c.m.}$	P_B	$\bar{E}_p=38.7$ MeV ϵ	P_2
10	23.3	0.369	0.010±0.001	0.028±0.004
22.5	26.2	0.360	0.012±0.003	0.033±0.010
25	29.0	0.368	−0.016±0.002	−0.043±0.006
27.5	31.9	0.350	−0.001±0.006	−0.003±0.018
30	34.8	0.371	−0.009±0.005	−0.023±0.013
32.5	37.7	0.358	−0.012±0.005	−0.034±0.014
35	40.5	0.369	−0.039±0.004	−0.106±0.011
40	46.1	0.369	−0.036±0.006	−0.097±0.016
45	51.8	0.368	−0.060±0.008	−0.163±0.022
50	57.3	0.369	−0.020±0.017	−0.053±0.045
52.5	60.1	0.365	−0.003±0.031	−0.008±0.085
55	62.8	0.374	0.023±0.023	0.061±0.063
60	68.3	0.377	0.131±0.027	0.347±0.071
62.5	71.0	0.360	0.290±0.036	0.806±0.108
65	73.7	0.373	0.214±0.025	0.574±0.067
70	79.0	0.371	0.285±0.030	0.768±0.081
75	84.3	0.370	0.287±0.026	0.776±0.070

TABLE III. p+Li polarization.

		Elastic+first excited state ($Q=-4.78$ MeV)			$\bar{E}_p=38.7$ MeV Second excited state ($Q=-4.63$ MeV)		
θ_{lab}	P_B	$\theta_{c.m.}$	ϵ	P_2	$\theta_{c.m.}$	ϵ	P_2
20	0.371	22.8	0.008±0.003	0.020±0.009	23.0	0.016±0.014	0.043±0.038
25	0.380	28.5	−0.003±0.003	−0.009±0.009	28.8	0.008±0.010	0.021±0.027
30	0.381	34.1	−0.002±0.004	−0.005±0.011	34.4	0.011±0.011	0.030±0.030
35	0.356	39.7	−0.019±0.006	−0.054±0.016	40.1	−0.020±0.011	−0.056±0.033
40	0.356	45.3	−0.027±0.006	−0.075±0.016	45.7	−0.016±0.009	−0.045±0.025
45	0.339	50.8	−0.036±0.008	−0.105±0.024	51.3	−0.022±0.010	−0.063±0.030
50	0.326	56.3	0.005±0.008	0.019±0.024	56.8	−0.029±0.008	−0.093±0.025
55	0.334	61.8	0.050±0.008	0.151±0.025	62.3	−0.064±0.008	−0.193±0.025
60	0.353	67.2	0.081±0.010	0.231±0.028	67.7	−0.045±0.008	−0.160±0.031
65	0.346	72.5	0.122±0.012	0.354±0.034	73.1	−0.042±0.012	−0.123±0.034
70	0.347	77.8	0.138±0.011	0.398±0.032	78.4	−0.010±0.013	−0.029±0.037
75	0.359	83.0	0.146±0.014	0.407±0.038	83.6	0.002±0.017	0.006±0.047
80	0.353	88.2	0.162±0.014	0.459±0.040	88.8	0.006±0.017	0.016±0.048
85	0.363	93.3	0.128±0.017	0.352±0.047	93.9	0.032±0.020	0.088±0.056
90	0.357	98.3	0.121±0.017	0.336±0.048	98.9	0.105±0.019	0.295±0.053
95	0.348	103.3	0.108±0.018	0.311±0.051	103.9	0.115±0.021	0.330±0.060
100	0.348	108.2	0.126±0.019	0.364±0.055	108.8	0.134±0.021	0.385±0.060

TABLE IV. p+C polarization.

		$C^{12}(p,p)C^{12}$			$\bar{E}_p=38$ MeV $C^{12}(p,p')C^{12*}$ ($Q=-4.433$ MeV)		
θ_{lab}	P_B	$\theta_{c.m.}$	ϵ	P_2	$\theta_{c.m.}$	ϵ	P_2
15	0.196	16.2	0.004±0.003	0.019±0.013	16.3	0.005±0.019	0.026±0.098
20	0.254	21.6	−0.003±0.002	−0.012±0.008	21.8	−0.027±0.015	−0.016±0.059
25	0.278	27.0	−0.020±0.003	−0.070±0.009	27.2	−0.035±0.012	−0.125±0.046
30	0.272	32.4	−0.025±0.003	−0.092±0.009	32.6	−0.066±0.011	−0.243±0.039
35	0.269	37.8	−0.028±0.003	−0.104±0.011	37.9	−0.070±0.010	−0.258±0.037
40	0.229	43.1	−0.017±0.007	−0.074±0.030	43.3	−0.082±0.015	−0.360±0.067
45	0.245	48.4	0.056±0.008	0.230±0.033	48.6	−0.052±0.012	−0.213±0.049
50	0.223	53.7	0.142±0.009	0.639±0.041	53.9	−0.041±0.016	−0.180±0.071
55	0.274	58.9	0.209±0.010	0.761±0.037	59.2	−0.061±0.016	−0.224±0.057
60	0.258	64.2	0.187±0.009	0.728±0.034	64.4	−0.028±0.017	−0.109±0.068
65	0.258	69.4	0.163±0.011	0.637±0.042	69.7	0.051±0.029	0.196±0.113
70	0.278	74.5	0.145±0.014	0.521±0.050	74.8	0.084±0.029	0.302±0.105
75	0.285	79.6	0.148±0.016	0.519±0.056	80.0	0.217±0.034	0.761±0.119
80	0.269	84.7	0.137±0.017	0.508±0.064	85.3	0.243±0.032	0.903±0.119
85	0.286	89.8	0.143±0.023	0.500±0.079	90.1	0.277±0.034	0.969±0.120

TABLE V. p+Al polarization.

			$\bar{E}_p=37.5$ MeV	
θ_{lab}	$\theta_{c.m.}$	ϵ	P_B	P_2
20	20.7	−0.028±0.003	0.284	−0.098±0.011
22.5	23.3	−0.051±0.005	0.303	−0.169±0.017
25	25.9	−0.064±0.008	0.269	−0.239±0.030
27.5	28.5	−0.077±0.004	0.299	−0.259±0.013
30	31.1	−0.056±0.006	0.288	−0.193±0.021
32.5	33.7	−0.072±0.008	0.299	−0.240±0.026
33.5	34.7	−0.040±0.014	0.284	−0.140±0.050
35	36.2	0.113±0.009	0.281	0.040±0.031
37.5	38.8	0.108±0.018	0.279	0.388±0.064
40	41.4	0.097±0.008	0.284	0.342±0.029
42.5	44.0	0.125±0.015	0.285	0.439±0.053
45	46.5	0.102±0.010	0.271	0.376±0.038
50	51.6	0.070±0.008	0.284	0.245±0.027
52.5	54.2	0.064±0.018	0.296	0.217±0.059
55	56.7	0.051±0.011	0.292	0.174±0.037
57.5	59.3	0.042±0.015	0.308	0.137±0.049
60	61.8	0.046±0.013	0.288	0.160±0.047
65	66.9	0.051±0.016	0.296	0.173±0.054
70	72.0	0.103±0.026	0.302	0.341±0.085
75	77.1	0.182±0.029	0.286	0.635±0.100
80	82.1	0.222±0.030	0.293	0.758±0.103

accordance with the Basel Convention.[15] Measured asymmetries are also given in these tables to facilitate the calculation of polarization at a later date in the event that the beam polarization was incorrectly determined (see section on determination of beam polarization). The errors given are due solely to counting statistics. Figures 6 through 12 give the variation of polarization versus scattering angle graphically. In Fig. 6 is also shown the theoretical predictions of Gammel and Thaler.[29] Because of insufficient resolution of the detectors used, contribution of the first and other low-lying excited states in elastic scattering could not be separated for aluminum, nickel, lead, and lithium[7] from the elastic scattering data.

IV. DISCUSSIONS

Of the various polarization measurements, only the p-He results were subjected to theoretical studies as

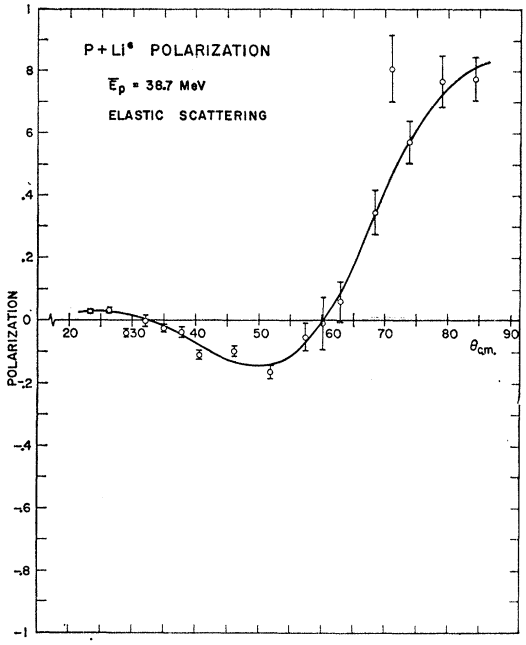

FIG. 7. p+Li^6 polarization, $\bar{E}_p$=38.7 MeV, elastic scattering.

reported in an earlier paper.[35] No further calculations have been reported on the discrepancy between theoretical predictions and measurements. From some preliminary studies, Thaler[36,36a] felt that this discrepancy between theoretical and measured values at large scattering angles may be a more serious nature than a simply misestimation of the magnitudes of the calculated parameters. He suggests that the trouble may be connected with the opening up of various inelastic channels in the scattering process, but a more quantitative statement must wait for a measurement of total reaction cross section at this incident proton energy.

TABLE VI. p+Ni polarization.

θ_{lab}	$\theta_{c.m.}$	ϵ	$\bar{E}_p$=38 MeV P_B	P_2
14	14.2	−0.014±0.002	0.320	−0.043±0.005
17.5	17.8	−0.037±0.003	0.328	−0.113±0.008
20	20.3	−0.069±0.005	0.289	−0.240±0.017
21	21.3	−0.105±0.004	0.324	−0.325±0.012
22.5	22.9	−0.115±0.005	0.302	−0.380±0.018
15	25.4	−0.128±0.009	0.278	−0.460±0.031
26	26.4	−0.120±0.011	0.301	−0.400±0.038
27	27.4	−0.051±0.010	0.320	−0.158±0.032
27.5	28.0	0.007±0.008	0.298	0.022±0.025
28	28.5	0.008±0.012	0.317	0.025±0.038
30	30.5	0.116±0.013	0.284	0.408±0.044
32.5	33.0	0.091±0.013	0.275	0.331±0.045
35	35.6	0.068±0.006	0.304	0.225±0.021
37.5	38.1	0.051±0.012	0.299	0.169±0.040
40	40.6	0.005±0.007	0.298	0.016±0.024
45	45.7	−0.032±0.009	0.291	−0.109±0.032
47.5	48.2	−0.064±0.014	0.328	−0.194±0.043
50	50.7	−0.079±0.015	0.282	−0.279±0.051
52.5	53.2	0.001±0.021	0.324	0.004±0.064
53	53.8	0.020±0.024	0.290	0.069±0.084
55	55.8	0.111±0.015	0.289	0.384±0.053
57.5	58.3	0.189±0.019	0.321	0.589±0.060
60	60.8	0.203±0.018	0.308	0.659±0.059
62.5	63.4	0.196±0.018	0.317	0.618±0.057
65	65.9	0.173±0.022	0.308	0.562±0.071
70	70.9	0.152±0.024	0.321	0.474±0.075

[35] C. F. Hwang, D. H. Nordby, S. Suwa, and J. H. Williams, Phys. Rev. Letters **9**, 104 (1962).

[36] R. M. Thaler (private communication).

[36a] *Note added in proof.* R. M. Thaler, C. C. Giamati, and V. A. Madsen, have submitted an analysis of p-He^4 results (to be published). A similar analysis has been made by S. Suwa and A. Yokosawa at Argonne National Laboratories.

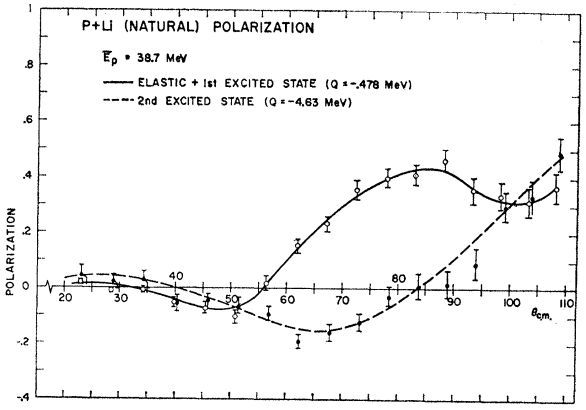

FIG. 8. p+Li (natural) polarization, $\bar{E}_p$=38.7 MeV.

TABLE VII. p+Pb Polarization

θ_{lab}	$\theta_{c.m.}$	ϵ	$\bar{E}_p$=37.5 MeV P_B	P_2
15	15.1	−0.004±0.002	0.277	−0.016±0.006
20	20.1	0.005±0.004	0.284	0.018±0.016
25	25.1	−0.002±0.007	0.284	−0.008±0.023
27.5	27.6	−0.034±0.011	0.283	−0.199±0.038
30	30.1	−0.040±0.014	0.294	−0.137±0.046
32.5	32.6	−0.013±0.011	0.285	−0.046±0.038
35	35.2	0.024±0.016	0.307	0.079±0.051
37.5	37.7	0.018±0.018	0.302	0.059±0.059
40	40.2	0.028±0.014	0.294	0.094±0.046
45	45.2	−0.042±0.023	0.280	−0.149±0.081
50	50.2	−0.070±0.021	0.270	−0.259±0.077
55	55.2	0.027±0.028	0.290	0.092±0.095

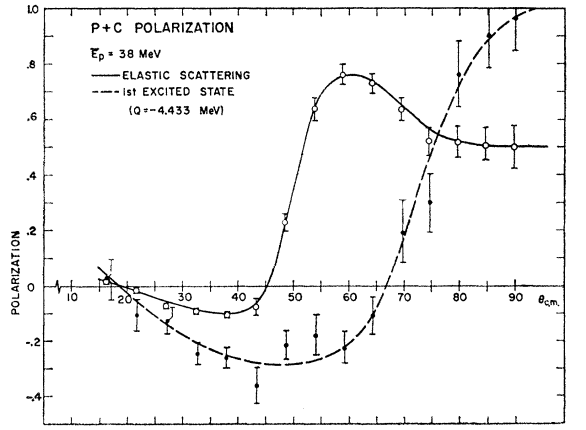

FIG. 9. p+C polarization, $\bar{E}_p$=38 MeV.

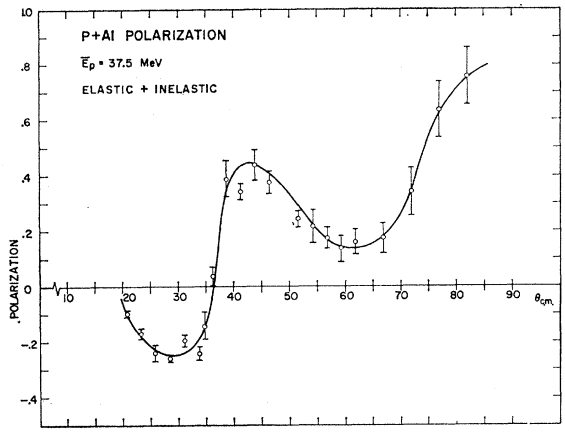

FIG. 10. p+Al polarization, $\bar{E}_p$=37.5 MeV.

Analyses of cross section and polarization data for optical-model parameter fits are now underway at Livermore and Oak Ridge.[37] The lithium measurements were motivated by similar measurements of Rosen *et al.*[38] It was felt that a comparison in polarization by various isotopes of a given element is of sufficient interest, and measurements utilizing counters would compliment Rosen's measurements at 14.5 MeV using emulsion plates. Unfortunately, due to a lack of isotopic targets of appropriate thicknesses, only lithium measurements were carried out. The comparison between the elastic scattering of Li^6 and Li^7 is further complicated by the very low first excited state of Li^7 ($Q=-0.48$ MeV) which was not resolved. Nevertheless, the polarizations from p-Li^7 interaction are comparable to those from p-Li^6 interaction for $\theta_{c.m.}$ less than 70° and is less than those from p-Li^6 interaction for $\theta_{c.m.}$ greater than 70°. Thus, qualitatively, the same isotope effect was found at 40 MeV as the findings of Rosen *et al.*,[38] for Li^6 and Li^7.

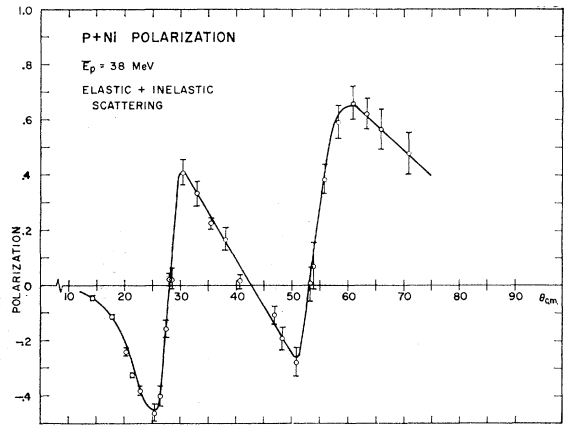

FIG. 11. p+Ni polarization, $\bar{E}_p$=38 MeV.

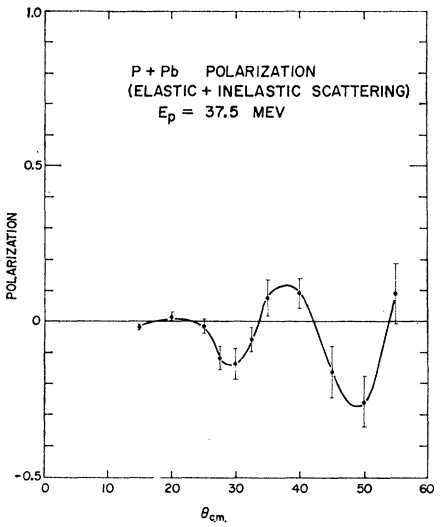

FIG. 12. p+Pb polarization, $\bar{E}_p$=37.5 MeV.

ACKNOWLEDGMENTS

We wish to thank R. P. Featherstone and the entire Linear Accelerator Laboratory personnel for their efforts to achieve peak performance of the linear accelerator during this experiment. Lawrence Williams collaborated in the development of the p-He polarimeter. Richard Gehrenbeck developed the high-resolution counters and helped in taking data.

[37] Erwin H. Schwarcz (Livermore), G. R. Satchler (Oak Ridge) (private communication).
[38] L. Rosen and W. T. Leland, Phys. Rev. Letters 8, 379 (1962).